

This article was downloaded by:

On: 25 January 2011

Access details: *Access Details: Free Access*

Publisher *Taylor & Francis*

Informa Ltd Registered in England and Wales Registered Number: 1072954 Registered office: Mortimer House, 37-41 Mortimer Street, London W1T 3JH, UK



Liquid Crystals

Publication details, including instructions for authors and subscription information:

<http://www.informaworld.com/smpp/title~content=t713926090>

Influence of the molecular structure of thermotropic liquid crystals on their ability to form monolayers at interface

Anna Modlińska^a; Krzysztof Ingot^a; Tomasz Martyński^a; Roman Dąbrowski^b; Jan Jadżyn^c; Danuta Bauman^a

^a Faculty of Technical Physics, Poznań University of Technology, Poznań, Poland ^b Institute of Chemistry, Military University of Technology, Warsaw, Poland ^c Institute of Molecular Physics, Polish Academy of Sciences, Poznań, Poland

To cite this Article Modlińska, Anna , Ingot, Krzysztof , Martyński, Tomasz , Dąbrowski, Roman , Jadżyn, Jan and Bauman, Danuta(2009) 'Influence of the molecular structure of thermotropic liquid crystals on their ability to form monolayers at interface', *Liquid Crystals*, 36: 2, 197 – 208

To link to this Article: DOI: 10.1080/02678290902759236

URL: <http://dx.doi.org/10.1080/02678290902759236>

PLEASE SCROLL DOWN FOR ARTICLE

Full terms and conditions of use: <http://www.informaworld.com/terms-and-conditions-of-access.pdf>

This article may be used for research, teaching and private study purposes. Any substantial or systematic reproduction, re-distribution, re-selling, loan or sub-licensing, systematic supply or distribution in any form to anyone is expressly forbidden.

The publisher does not give any warranty express or implied or make any representation that the contents will be complete or accurate or up to date. The accuracy of any instructions, formulae and drug doses should be independently verified with primary sources. The publisher shall not be liable for any loss, actions, claims, proceedings, demand or costs or damages whatsoever or howsoever caused arising directly or indirectly in connection with or arising out of the use of this material.

Influence of the molecular structure of thermotropic liquid crystals on their ability to form monolayers at interface

Anna Modlińska^a, Krzysztof Ingot^a, Tomasz Martyński^a, Roman Dąbrowski^b, Jan Jadżyn^c and Danuta Bauman^{a*}

^aFaculty of Technical Physics, Poznań University of Technology, Nieszawska 13a, 60-965, Poznań, Poland; ^bInstitute of Chemistry, Military University of Technology, S. Kaliskiego 1, 00-950 Warsaw, Poland; ^cInstitute of Molecular Physics, Polish Academy of Sciences, M. Smoluchowskiego 17, 60-179, Poznań, Poland

(Received 20 November 2008; final form 19 January 2009)

Langmuir and Langmuir–Blodgett (LB) films of some thermotropic liquid crystals of rod-like shape have been studied. It has been found that the compounds with the terminal isothiocyanato (–NCS) group are not able to form a compressible monolayer at the air–water interface. Very short and very long alkyl or alkoxy chains attached to the rigid molecular core also hinder the creation of the stable films. The Langmuir films have been characterised by the surface pressure–area and surface potential–area isotherms and by Brewster angle microscopy (BAM). The analysis of the isotherms and the BAM images suggests that the organisation of the mesogenic molecules on the water surface is dependent on their structure and to some extent reflects their ability to form an appropriate mesophase in the bulk. For the LB films of the liquid crystals the electronic absorption spectra have been recorded. On the basis of these spectra the conclusions about the creation of the self-aggregates by mesogenic molecules at the air–solid substrate interface have been drawn. The polarised absorption spectra have allowed one to determine the alignment of molecules on the quartz surface.

Keywords: liquid crystal; Langmuir film; Langmuir–Blodgett film; absorption spectroscopy

1. Introduction

It is well known that in liquid crystal displays (LCDs) macroscopic homogeneous orientation within layers of few micrometers in thickness is necessary (1). Such orientation can be induced by the surface through the anchoring of the liquid crystal molecules (2). As the surface interactions play a significant role in LCD designing, the knowledge of these interactions is of primary importance. Very simple systems in which surface interactions, as well as intermolecular interactions, can be easily investigated are gas–liquid and gas–solid interfaces that provide us with a unique method to study matter in the form of layers with a thickness of the order of the molecular dimension (3–6). The monolayers at air–water (Langmuir films) and air–solid (Langmuir–Blodgett (LB) films) interfaces are generally formed by amphiphilic molecules, thus it is not astonishing that they can be formed of lyotropic liquid crystals. Thermotropic liquid crystal molecules cannot be directly treated as amphiphilic, nevertheless many of them are able to create stable compressible monolayers at the liquid surface, which can be next transferred at the solid substrates (7–14).

Among calamitic liquid crystals, the most intensively investigated were compounds composed of the molecules consisting of the alkyl chain attached to the rigid core of aromatic or aliphatic rings connected with the polar group. So, in such a molecular

structure, one can distinguish hydrophobic (alkyl chain) and hydrophilic (polar group) parts. This latter part comes into contact with the water enabling creation of the Langmuir film. Some members of the homologous series of 4-*n*-alkyl-4'-cyano-biphenyls (*n*CB) are classical examples of thermotropic calamitic liquid crystals, which are able to form stable monolayers at the water surface (7, 9–14). The most comprehensive investigations were carried out for 4-octyl-4'-cyano-biphenyl (8CB) (7, 9–14). Using Brewster angle microscopy (BAM) (15, 16), it was found that the monolayer of 8CB collapses reversibly to the trilayer and the multilayer during the compression process (10, 11, 13). The ability for the creation of Langmuir films that also exhibit other homologues from the *n*CB series was found by Daniel *et al.* (7) and Ingot *et al.* (14) for the compounds with *n* = 4–12. On the basis of the surface pressure versus area per molecule isotherm measurements and the BAM images, Ingot *et al.* (14) suggested that the organisation of the liquid crystal molecules on the water surface beyond the collapse is to some extent correlated with their ability to form corresponding mesophases in the bulk; nematogenic compounds tend to form rounded droplet-like domains with the nematic order of molecules, whereas the smectogenic compounds tend to form interdigitated bilayers, such as in the smectic A_d phase (17).

*Corresponding author. Email: bauman@phys.put.poznan.pl

In this paper, we have studied Langmuir and LB films formed by thermotropic calamitic liquid crystals, often used as components for the preparation of liquid crystal mixtures for LCDs. The aim of our study is to recognise the relationship between the molecular structure of mesogens and the stability of monolayers formed by them at interfaces. We also tried to explore to what extent the order in nematic and smectic phases is preserved in monomolecular layers.

2. Experimental

The liquid crystal materials from the homologous series of 4-*n*-alkoxy-4'-cyanobiphenyl (*n*OCB), 4-*n*-alkyl(4'-cyanophenyl)benzoate (*n*CPB), 4-*n*-alkyl-4'-cyanobiphenyl (*n*CB), *trans*-4-*n*-alkyl(4'-cyanophenyl)-hexane (*n*PCH), 4-(*trans*-4'-*n*-alkylcyclohexyl)-isothiocyanato-benzene (*n*CHBT), and *n*-alkyl-4-(4'-isothio-

cyanato-phenyl)bicyclo[2,2,2]-octanes (*n*BOBT) were investigated. Additionally, the study for two novel synthesised compounds, namely 4-cyano-3-fluorophenyl 4'-*n*-octyloxybenzoate (8OCFPB) and 4-cyano-phenyl 4'-*n*-octyloxy-2-fluoro-benzoate (8OCPFB), was carried out. The molecular structure of the liquid crystal materials investigated is given in Figure 1. All compounds were synthesised and chromatographically purified at the Institute of Chemistry, Military University of Technology, Warsaw (Poland). The phase transition temperatures in the bulk, determined on the basis of textures observed by means of a polarising microscope equipped with a hot stage, were in agreement with the data given in the literature (14, 17–20). Most of the liquid crystals under investigation have only a nematic (N) phase between the solid and isotropic phases. 8CB, 9CB, 8OCB, 9OCB and 10PCH have both nematic and smectic A (SmA) phases, while

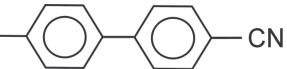





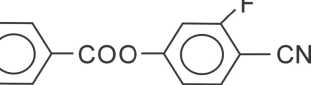
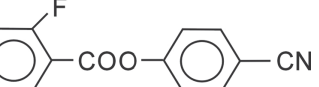
Abbreviation	Molecular structure	<i>n</i> for compounds investigated
<i>n</i> OCB	$C_nH_{2n+1}-O-$  $-CN$	4–9
<i>n</i> CPB	$C_nH_{2n+1}-$  $-CN$	4–10
<i>n</i> CB	$C_nH_{2n+1}-$  $-CN$	2–14
<i>n</i> PCH	$C_nH_{2n+1}-$  $-CN$	2–12
<i>n</i> CHBT	$C_nH_{2n+1}-$  $-NCS$	3–9
<i>n</i> BOBT	$C_nH_{2n+1}-$  $-NCS$	5–8
8OCFPB	$C_8H_{17}-O-$  $-CN$	8
8OCPFB	$C_8H_{17}-O-$  $-CN$	8

Figure 1. Molecular structure of liquid crystals investigated.

10CB to 14CB and 12PCH show only the SmA phase. The phase sequence for fluoro-compounds is as follows:

8OCFPB Cr • 53.5°C • N • 56.3°C • Iso

8OCPFB Cr • 58.4°C • N • 65.4°C • Iso

Langmuir and LB films were prepared in a Minitrough 2 (KSV Instruments Ltd., Finland). The mesogens were first dissolved in chloroform (Uvasol, for spectroscopy, E. Merck) to stock concentrations of 0.1 mM and kept refrigerated. Next, the appropriate solution was spread onto the deionised water subphase to form a monolayer and was equilibrated for about 15 minutes to allow the solvent to evaporate. A constant subphase temperature was maintained by a cooling circulator and kept constant at 20°C.

The most basic characterisation of Langmuir films is the measurement of the surface pressure versus the average area available for one molecule isotherm (π - A isotherm) (3-6). For monolayers, π is defined as the surface tension of the pure subphase minus the surface tension of the subphase-monolayer system. In our experiment the monolayer was compressed symmetrically from both sides at a barrier motion speed of 5 mm min⁻¹ (approximately 2×10^{-7} nm² molecule⁻¹ s⁻¹), while the surface pressure was monitored by a platinum Wilhelmy plate balance with an accuracy of ± 0.1 mN m⁻¹. Additionally, the surface potential (ΔV) of the monolayer as a function of the mean molecular area (ΔV - A isotherm) was measured using the vibrating plate method by means of a SPOT 1 head from KSV. The accuracy of this method was ± 1.0 mV. ΔV is defined as the difference in the potential between a monolayer-covered surface and a clean subphase surface (3). All measurements were repeated on fresh subphases three to five times to confirm reproducibility. The standard trough cleaning procedure was adopted between measurements. Further experimental details about Langmuir film preparation are given elsewhere (12).

The texture of the films at the air-water interface was visualised by means of a Brewster angle microscope. The instrument we used is based on the Hoenig and Moebius setup (15) and was built in our laboratory. The image features were observed with a lateral resolution of ≈ 5 μ m.

For LB film fabrication, polished quartz plates ($35 \times 10 \times 1$ mm³) were used as the solid substrates with the hydrophilic surface. The vertical dipping method was used and the dipping rate was 5 mm min⁻¹. Langmuir films, kept at a constant surface pressure, were transferred onto quartz plates at the surface pressure below the collapse point, which

corresponds to the stage of the formation of the compressed monolayer. The dipping stroke was 25 mm. The transfer ratio was estimated by calculating the ratio of the decrease in the subphase area to the area on the substrate coated by the layer. Values between 1.00 and 1.20 were obtained. Successful deposition of the mesogens investigated took place only on the first up-stroke of the substrate. For the LB films obtained the absorption spectra were recorded in the ultraviolet-visible spectroscopy (UV-Vis) region by means of a spectrophotometer Varian CARY 400.

3. Results and discussion

3.1. Characterisation of Langmuir films

The amphiphilic character of calamitic liquid crystals is not a sufficient condition for the formation of stable and compressible monolayers at the air-water interface. Previously (13, 21) it was found that 4-(*trans*-4'-octylcyclohexyl)isothiocyanato-benzene (8CHBT) and 4-octyl-4'-isothiocyanato-biphenyl (8BT) are examples of compounds that are unable to form a homogeneous monomolecular layer when they are spread onto a water subphase. From our present study it follows that all the members of the homologous series of *n*CHBT, as well as the mesogens from the *n*BOBT series, gave a monolayer that did not resist barrier compression; the molecules were expelled and the formation of an irregular phase was observed. All these compounds have the terminal isothiocyanato (-NCS) group and it seems that already this group makes the formation of the Langmuir film impossible. The other liquid crystals under investigation have the terminal cyano (-CN) group. Among them only those with very short and very long alkyl or alkoxy chains could not form a stable monolayer.

Figures 2 and 3 show the π - A isotherm diagrams, obtained during the compression process for those members of, respectively, the *n*OCB and *n*CPB series that are able to create the Langmuir film on the water surface. With a decrease of the available area, the surface pressure rises up to the collapse point at appropriate π_C and A_C values (the collapse point is recognised as the point in the π - A isotherm where the ratio $\partial\pi/\partial A$ begins to decrease due to the next phase transition), indicating the formation of the condensed monolayer. However, the collapse point occurs at the mean molecular area, which is larger than the theoretical molecular cross-section (≈ 0.20 nm²). This effect can be explained in terms of strong repulsive interactions between the electric dipoles of the cyano groups. As a result of such interactions, the molecules in the monolayer are not densely packed and are tilted with respect to the water surface. The average tilt angle can be estimated by assuming that the mean molecular

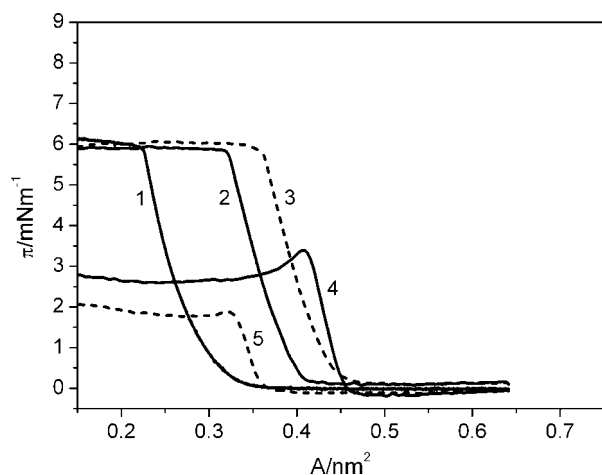


Figure 2. Surface pressure-area isotherms of Langmuir films formed from 5OCB (1), 6OCB (2), 7OCB (3), 8OCB (4), and 9OCB (5).

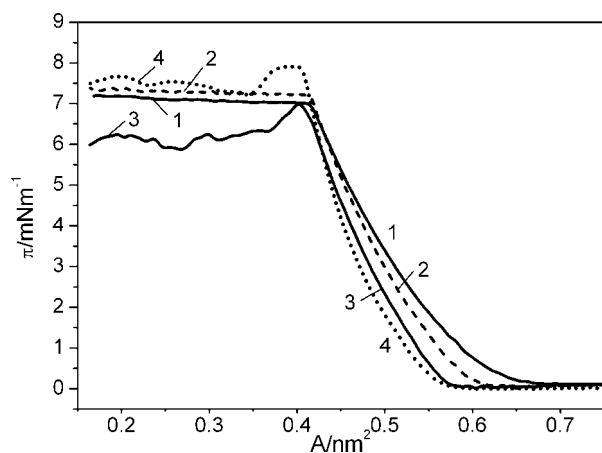


Figure 3. Surface pressure-area isotherms of Langmuir films formed from 6CPB (1), 7CPB (2), 8CPB (3), and 9CPB (4).

area is determined only by the rigid core of the liquid crystal molecule and taking into account the experimental value of A_C . Behind the collapse point, the π - A isotherms of 5OCB, 6OCB, 7OCB, 6CPB and 7CPB exhibit a broad plateau, and the expansion isotherms show only a slight hysteresis with respect to the compression ones. This highlights the high stability of the film created. The steepness of the isotherm increases with increasing alkoxy or alkyl chain length, indicating some improvement of the monolayer rigidity, however the collapse pressure remains constant. In the case of 8OCB, 9OCB, 8CPB and 9CPB, behind the collapse point in the π - A isotherm, a 'spike', i.e. a rapid fall of the surface pressure, appears and a large hysteresis of expansion and compression isotherms is observed. This implies the instability of the monolayers and

leads to the conclusion that the chain with $n \geq 8$ carbon atoms in the molecules of the n OCB and n CPB series is too long to maintain the stability of the Langmuir films.

Further information about molecular organisation, particularly at the early stages of the film compression when the surface pressure is still zero, can give the surface potential-area isotherm. The surface potential can be related to an average effective dipole moment for the monolayer-forming molecules by the Helmholtz equation (22, 23):

$$\Delta V = \mu_{\perp} / A \epsilon_r \epsilon_0, \quad (1)$$

where $\mu_{\perp} = \mu \cos \gamma$ (γ is the angle between the surface normal and the dipole axis) is the average vertical component of the molecular dipole moment, A is the mean area per molecule, and ϵ_r and ϵ_0 are the dielectric constant of the monolayer and the electric permittivity of the free space, respectively.

Figure 4 (reproduced from (24)) presents an electric surface potential-area isotherm (solid curve), recorded simultaneously with the π - A isotherm (dotted curve), as well as the effective dipole moment-area isotherm (dashed curve) for the liquid crystal 8CB, which can be treated as a reference for the compounds studied here. Such isotherms were obtained for all the mesogens under investigation and some examples of the results for representatives of n OCB, n CPB, n CB and n PCH are shown in Figures 5-7, respectively, whereas Tables 1 and 2 collect the features of π - A and ΔV - A isotherms of the monolayers of all members of these series that are able to form the compressible Langmuir film. A_0^{π} and $A_0^{\Delta V}$ are the values of the area at which, respectively, the surface pressure, π , and the surface potential, ΔV ,

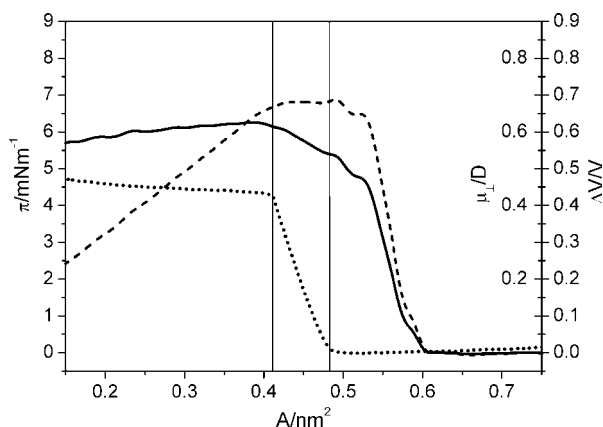


Figure 4. Surface potential, ΔV (solid curve), surface pressure, π (dotted curve) and effective dipole moment, μ_{\perp} (dashed curve) as a function of the mean molecular area, A for Langmuir film of 8CB.

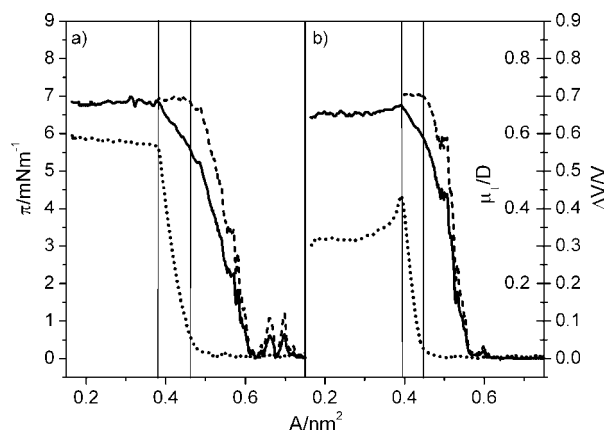


Figure 5. Surface potential, ΔV (solid curve), surface pressure, π (dotted curve) and effective dipole moment, μ_{\perp} (dashed curve) as a function of the mean molecular area, A for Langmuir films of 7OCB (a) and 8OCB (b).

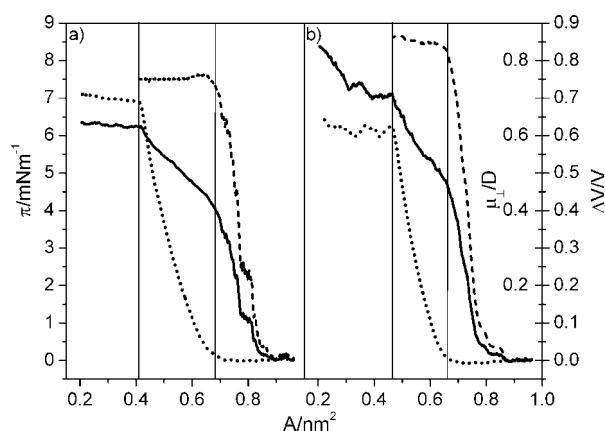


Figure 6. Surface potential, ΔV (solid curve), surface pressure, π (dotted curve) and effective dipole moment, μ_{\perp} (dashed curve) as a function of the mean molecular area, A for Langmuir films of 6CPB (a) and 8CPB (b).

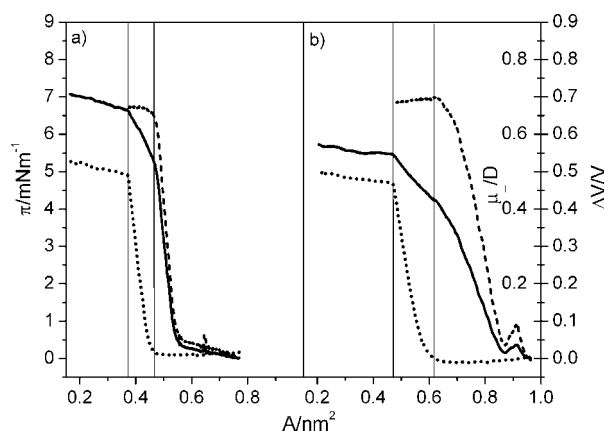


Figure 7. Surface potential, ΔV (solid curve), surface pressure, π (dotted curve) and effective dipole moment, μ_{\perp} (dashed curve) as a function of the mean molecular area, A for Langmuir films of 7CB (a) and 7PCH (b).

start to increase. φ is the angle between the normal to the water surface and the long molecular axis (Figure 8). Given in tables the values of φ as well as those of μ_{\perp} were calculated at the collapse pressure. The detailed analysis of π - A isotherms of Langmuir films of the liquid crystals from the n CB and n PCH series (Table 2) was made in (14), and here we present additional results of the surface potential measurements.

From the isotherm runs presented in Figures 5–7 it follows that the shape of the ΔV - A isotherms for all the liquid crystals investigated is quite similar. In all the cases the rise of ΔV is observed earlier than the rise of π . ΔV first increases rather sharply up to the area that coincides with the onset area for π . Next, ΔV keeps on growing, but at a slower rate and reaches the maximum at the collapse point of the π - A isotherm. The effective dipole moment, μ_{\perp} , rises together with the rise of ΔV up to the highest value being reached at the area corresponding to the onset for the surface pressure. Such a value of μ_{\perp} remains almost constant up to the collapse point (the product $\Delta V \cdot A$ is constant in the region between the vertical lines in Figures 4–7). The runs of μ_{\perp} - A isotherms indicate that at the large area available for the liquid crystal molecules, they lie almost horizontally at the water surface. Upon compression, the molecules start to interact and at some critical area the hydrophobic parts of them lift up from the water surface, causing their tilted alignment with respect to the horizontal direction. Such orientational changes are confirmed by the significant increase of ΔV and μ_{\perp} at this stage. Since μ_{\perp} reaches the maximal value at the area where the surface pressure starts to increase and then remains constant up to the collapse point, we suppose that the molecular orientation does not change. This means that the tilt angle of the mesogenic molecules at the air–water interface is settled already at the beginning of the formation of the condensed monolayer.

From Figure 4 it follows that behind the collapse point, μ_{\perp} of 8CB in the Langmuir film decreases. This is not reasonable, because for this liquid crystal in the region of $A < A_C$, the creation of the interdigitated bilayer with antiparallel aligned molecules is assumed (9, 11). Thus, μ_{\perp} should remain constant. In fact, μ_{\perp} calculated directly from Equation (1) has no physical meaning in this region of A . The surface potential is contributed further only by the first monolayer coming into contact with the water. Since the dipole density in this layer does not change during reduction of the mean molecular area, ΔV stays constant. For other liquid crystals investigated, the constant value of ΔV beyond the collapse point is also observed, leading to the conclusion that the molecules have to be ‘pushed out’ above the monolayer surface and align

Table 1. Features of π - A and ΔV - A isotherms, the average angle between the long molecular axis and the normal to the water surface, φ , and the effective dipole moment, μ_{\perp} , for Langmuir films of members of the homologous series of n OCB and n CPB.

Compound	A_0^{π}/nm^2	A_C/nm^2	π_C/mNm^{-1}	$\varphi/^\circ$	$A_0^{\Delta V}/\text{nm}^2$	$\Delta V_C/\text{V}$	μ_{\perp}/D
5OCB	0.34	0.22	5.8	24	0.44	0.611	0.40
6OCB	0.45	0.32	5.8	36	0.61	0.643	0.54
7OCB	0.45	0.36	5.8	41	0.62	0.683	0.69
8OCB	0.44	0.40	3.6	47	0.57	0.675	0.70
9OCB	0.38	0.33	1.9	37	- ^a	- ^a	- ^a
6CPB	0.67	0.42	7.0	46	0.88	0.624	0.75
7CPB	0.62	0.42	7.2	46	0.77	0.624	0.75
8CPB	0.62	0.40	6.2	43	0.85	0.710	0.87
9CPB	0.57	0.41	7.8	45	0.83	0.740	0.81

^a ΔV - A isotherm impossible to record

Table 2. Features of π - A and ΔV - A isotherms, the average angle between the long molecular axis and the normal to the water surface, φ , and the effective dipole moment, μ_{\perp} , for Langmuir films of members of the homologous series of n CB and n PCH.

Compound	A_0^{π}/nm^2	A_C/nm^2	π_C/mNm^{-1}	$\varphi/^\circ$	$A_0^{\Delta V}/\text{nm}^2$	$\Delta V_C/\text{V}$	μ_{\perp}/D
4CB	0.29	0.20	4.3	25	0.41	0.590	0.31
5CB	0.39	0.30	4.8	39	0.60	0.610	0.48
6CB	0.45	0.36	5.3	49	0.57	0.618	0.58
7CB	0.46	0.37	5.0	51	0.56	0.663	0.65
8CB	0.47	0.41	4.8	60	0.65	0.630	0.67
9CB	0.46	0.40	4.6	57	0.54	0.619	0.65
10CB	0.51	0.44	4.4	68	0.58	0.683	0.79
11CB	0.47	0.40	4.6	57	0.64	0.744	0.94
12CB	0.49	0.43	4.6	65	0.72	0.787	0.90
4PCH	0.61	0.42	6.0	45	0.95	0.502	0.56
5PCH	0.59	0.45	5.4	50	0.90	0.534	0.64
6PCH	0.58	0.45	5.3	50	0.65	0.551	0.67
7PCH	0.61	0.47	4.8	53	0.86	0.544	0.68
8PCH	0.57	0.48	5.3	54	0.71	0.520	0.73
9PCH	0.54	0.47	4.6	53	0.73	0.589	0.73
10PCH	0.53	0.47	3.5	53	0.72	0.649	0.81

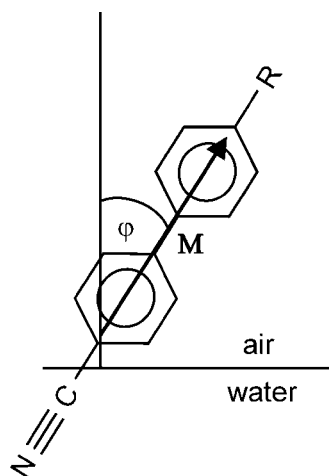


Figure 8. Definition of the φ angle between the normal to the water surface and the long molecular axis (when instead of water the surface is quartz slide, this angle is marked as β).

on the top of the homogeneous monolayer. The alignment of molecules in this region will be discussed later.

Figures 9 and 10 show the π - A , ΔV - A , and μ_{\perp} - A isotherms for the monolayers of liquid crystals 8OCFPB and 8OCPFB, respectively, whereas in Table 3 the characteristic parameters of isotherms are gathered. These two liquid crystals differ only in the position of the lateral fluorine atom attached to one of the benzene rings. However, this small difference significantly affects the behaviour of the molecules in the Langmuir films. Although both compounds are able to make the compressible monolayer, which collapses at the same A_C , only the monolayer of 8OCFPB is stable, which is confirmed by very slight hysteresis between the compression and expansion isotherms. In the case of 8OCPFB, not only the 'spike', but also a large hysteresis for π - A isotherms was observed. The differences also occur in the run of

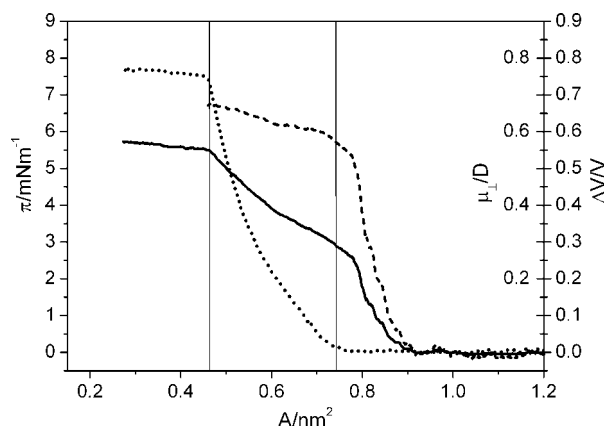


Figure 9. Surface potential, ΔV (solid curve), surface pressure, π (dotted curve) and effective dipole moment, μ_{\perp} (dashed curve) as a function of the mean molecular area, A for Langmuir film of 8OCFPB.

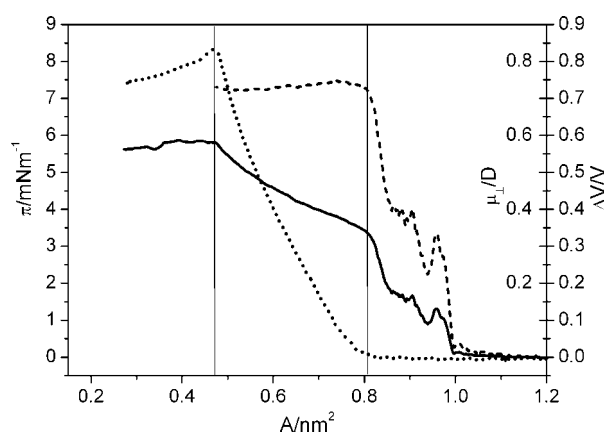


Figure 10. Surface potential, ΔV (solid curve), surface pressure, π (dotted curve) and effective dipole moment, μ_{\perp} (dashed curve) as a function of the mean molecular area, A for Langmuir film of 8OCPFB.

ΔV - A and μ_{\perp} - A isotherms. The region of the gentle increase of ΔV with decreasing A for 8OCFPB begins earlier than the onset of π and, as a consequence, μ_{\perp} changes up to the collapse point. This means that during formation of the condensed monolayer the molecules assume more and more vertical alignment leading to the increasing value of μ_{\perp} . Contrary to this, μ_{\perp} for 8OCPFB remains constant in the whole region

of the surface pressure increase, similar to that observed for other liquid crystals investigated.

Let us now compare the values of μ_{\perp} obtained for the various liquid crystals under investigation. It should be kept in mind that the quantity μ_{\perp} is a so-called apparent dipole moment and cannot be mistaken for the dipole moment of an isolated molecule, because it is influenced by several dipole fields. According to the Demchak-Fort model (25), μ_{\perp} is composed of three independent contributions arising from (i) orientation of water dipoles in the vicinity of the headgroup, (ii) the headgroup dipoles, and (iii) the hydrophobic part dipoles. Moreover, in our calculations we assumed, as is customary (26, 27), that $\epsilon_r = 1$, although it is known that dipoles in a monolayer may be embedded in media with a distinct dielectric constant value (28, 29). However, all liquid crystals considered are embedded in the same subphase and all have the terminal -CN group with the dipole moment equal to ≈ 4 D (30). Thus, we are able to trace the influence of the other part of the molecules on the μ_{\perp} value, even if we cannot determine the absolute value of it. Looking at the data given in Tables 1 and 2 we can see the following indications: (i) an addition of the ester group, having a dipole moment equal to ≈ 2.5 D (30), as the bridge between two benzene rings causes a significant increase of the μ_{\perp} value (compare the liquid crystals from the n CPB and n CB series with the same n); (ii) the cyclohexane ring has a slightly greater contribution to μ_{\perp} than the benzene rings (compare liquid crystals from the n CB and n PCH series), and (iii) the addition of an oxygen atom to the alkyl chain to some extent influences the μ_{\perp} value, although the changes are dependent on the chain length (compare liquid crystals from the n CB and n OCB series). From the data given in Table 3 it follows that the position of the fluorine atom (the dipole moment μ of the C-F group is ≈ 1.5 D (30)) in the molecule considerably affects the effective dipole moment. The value of μ_{\perp} for 8OCFPB is very similar to those of the compounds from the n CPB series, meaning that the fluorine atom does not significantly influence the alignment of molecules on the water surface, because it does not interact directly with the water. Contrary to this, when the fluorine atom in 8OCFPB is close to the -CN group, it can interact with the water causing changes to the

Table 3. Features of π - A and ΔV - A isotherms, the average angle between the long molecular axis and the normal to the water surface, φ , and the effective dipole moment, μ_{\perp} , for Langmuir films of 8OCFPB and 8OCPFB.

Compound	A_0^{π}/nm^2	A_C/nm^2	π_C/mNm^{-1}	$\varphi/^\circ$	$A_0^{\Delta V}/\text{nm}^2$	$\Delta V_C/\text{V}$	μ_{\perp}/D
8OCFPB	0.72	0.45	7.4	40	0.91	0.551	0.67
8OCPFB	0.76	0.45	8.3	40	1.02	0.577	0.73

value and the direction of the resultant dipole moment. As a result the μ_{\perp} value may decrease.

Additional information about the organisation of molecules at the air–water interfaces gives the BAM, which enables the direct observation of the texture of Langmuir films. It was found that up to the collapse point all mesogens behaved similarly. Immediately after the spreading of the solution, the formation of condensed monolayer islands in the floating film could be observed. As the surface pressure was raised, the islands packed together into a completely compressed monolayer, giving a homogeneous picture (data not shown). Just after the collapse point, in the plateau region, BAM images for various liquid crystals were very different. The texture of compounds from the *n*CB and *n*PCH homologous series is described in detail in (14). The correlation between BAM images and the ability of the liquid crystals to form a corresponding mesophase was found. Whereas for smectogens (8CB, 9CB and 10CB) only optically flat domains were found and the Langmuir films of most nematogens (4CB, 5CB, *n*PCH series) were characterised by the existence of three-dimensional lens-shaped domains. The textures of the monolayers formed by nematogenic 6CB and 7CB were intermediate between those of 8CB–10CB and of the aforementioned nematogens. Up to $A \approx 0.14 \text{ nm}^2$ the domains characteristic for smectogenic compounds were observed. As an example, Figure 11(a) presents the BAM image for 7CB at $A = 0.17 \text{ nm}^2$. However, further compression caused the creation of objects very similar to those found for other nematogens. This effect was explained in terms of the existence of some groups of molecules in the 6CB and 7CB monolayers, which are early precursors of the appearance of the smectic order in the next members of the homologous series.

Among the liquid crystals from the *n*OCB series, only 8OCB and 9OCB are smectogenic. Unfortunately, the Langmuir films formed by them are unstable. The BAM image for 8OCB at $A = 0.15 \text{ nm}^2$ is shown in Figure 11(b). Instead of the flat domains as in the case of 8CB–10CB, we see the irregular strips. Similar images were obtained for 9OCB, 8CPB and 9CPB. At some areas in the Langmuir films of these liquid crystals, white objects with different shapes could also be registered, as was found for the liquid crystals from the *n*CB and *n*PCH series, creating unstable monolayers at the air–water interface (14). However, for 7OCB we could record the images that were, at least partially, quite similar to those for 6CB and 7CB and an example of this at $A = 0.19 \text{ nm}^2$ is presented in Figure 11(c). Figure 11(d) shows the BAM image for the liquid crystal 7CPB recorded at $A = 0.41 \text{ nm}^2$, i.e. just after the collapse point. We can observe the appearance of the domains of quite high brightness surrounded by interference

rings. With the decrease of the A value, the number of the domains rises. However, they are not in collision and do not join together. The picture is very similar to pictures for nematogens from the *n*CB and *n*PCH series (14). Thus, we deal here with three-dimensional droplet-like domains. Such images were also obtained for 6CPB, 5OCB, and 8OCFPB (Figure 11(e)). The only difference was in the size and the number of the domains at the same mean molecular area. Figure 11(f) presents the BAM image of 8OCFPB recorded at $A = 0.31 \text{ nm}^2$. The picture presented here shows the irregular object, which is characteristic for unstable Langmuir films.

3.2. Electronic absorption spectra of LB films

Figure 12 shows the absorption spectra of the monolayer-LB films of the chosen liquid crystals recorded in the ultraviolet (UV) region from 225 nm to 350 nm, whereas in Table 4 the position of the absorption maximum, λ_{max} , and the half-bandwidth of the absorption band, δ , for the liquid crystals under investigation as LB films are presented. For comparison, Table 5 gathers the values of λ_{max} and δ for the liquid crystals with eight carbon atoms in the alkyl or alkoxy chain dissolved in chloroform at the concentration of $3.2 \cdot 10^{-5} \text{ mol dm}^{-3}$. The data for 8CB and 8OCB are in good agreement with those given in the literature (31–33), whereas those of 8CPB, 8OCFPB and 8OCFPB, to our best knowledge, are presented here for the first time. The absorption maximum of the liquid crystals from the *n*PCH series appears outside the spectral region used in the experiment ($< 225 \text{ nm}$). It follows from the data presented here that both the absorption band position and the bandwidth strongly depend on the molecular structure of the liquid crystals. The presence of the ester group between the benzene rings causes the hypsochromic displacement of the λ_{max} value, whereas the addition of the oxygen atoms in the terminal chain shifts the absorption band towards longer wavelengths. The position of the fluorine atoms strongly affects both the λ_{max} and δ values.

Comparing the data from Tables 4 and 5, it can be seen that the wavelengths of the absorption band maximum of the liquid crystals in the LB film are almost the same as in the diluted solution. However, the half-bandwidths in the LB film are significantly larger than those in the chloroform. As in the chloroform the measurements were made at very low liquid crystal concentration, it is clear that the absorption spectra obtained are characteristic for monomers. Thus, the broadening of the spectra of the LB films could be attributed to the creation of some kind of aggregates between the liquid crystal molecules, although the influence of the surface interaction cannot be excluded.

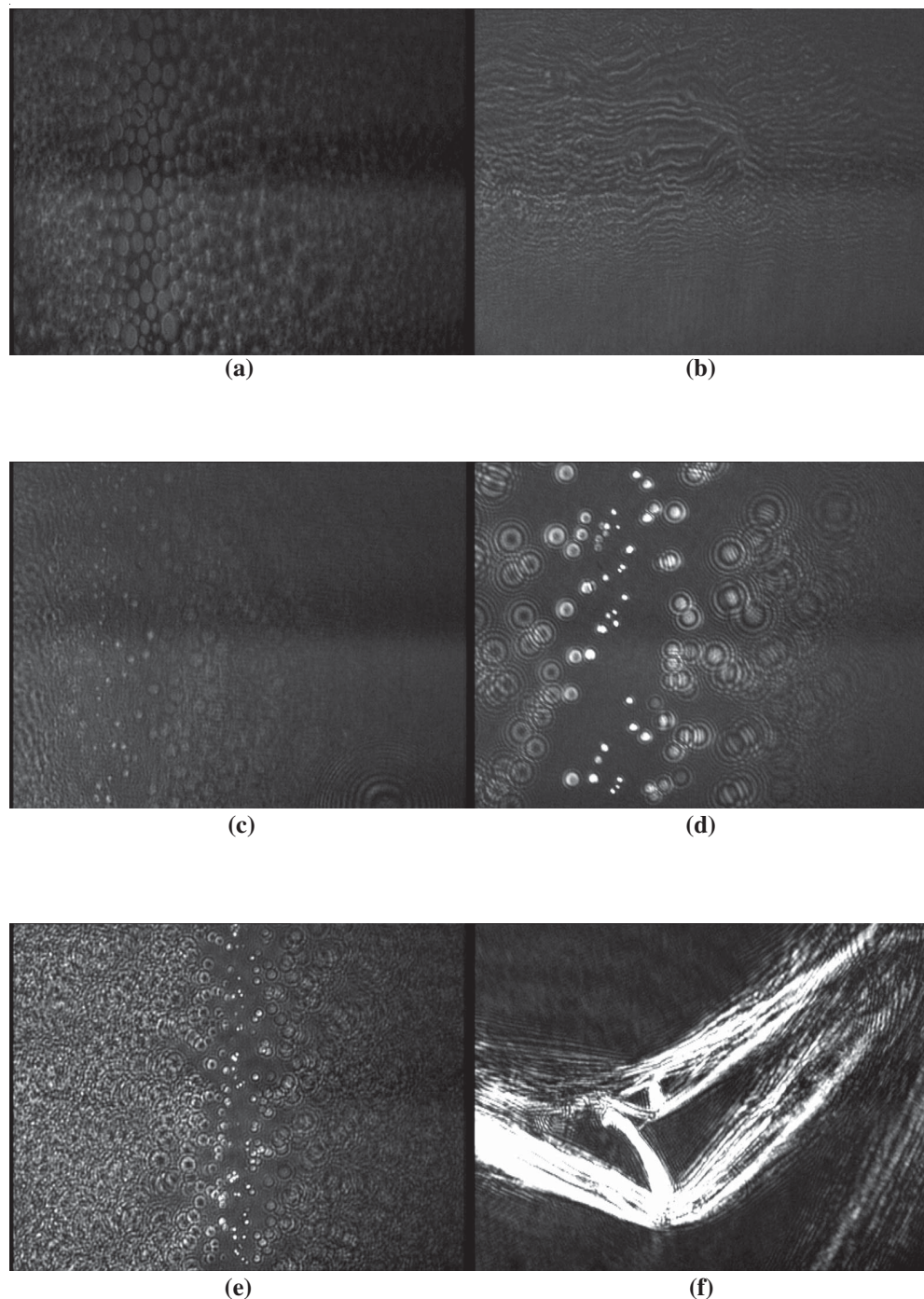


Figure 11. BAM images obtained during the compression of the Langmuir film of: (a) 7CB at $A = 0.17 \text{ nm}^2$; (b) 8OCB at $A = 0.15 \text{ nm}^2$; (c) 7OCB at $A = 0.19 \text{ nm}^2$; (d) 7CPB at $A = 0.41 \text{ nm}^2$; (e) 8OCFPB at $A = 0.36 \text{ nm}^2$; and (f) 8OCPFB at $A = 0.31 \text{ nm}^2$.

The creation of aggregates without spectral shift is a peculiar phenomenon, but it is predicted by the molecular exciton model proposed by Kasha *et al.* (34). According to this model, if sufficiently strong electronic transitions exist, dipole–dipole interactions in molecular aggregates result in the splitting of the energy level of the excited state into two levels with

higher and lower energy relative to the undisturbed excited state. The molar extinction coefficient of the liquid crystals investigated is quite large, over 26,000 (Table 5), thus the exciton coupling is most likely to occur in compressed monolayers. Assuming the parallel configuration of molecules in the simplest aggregate, i.e. in dimer, the co-planar arrangement of the

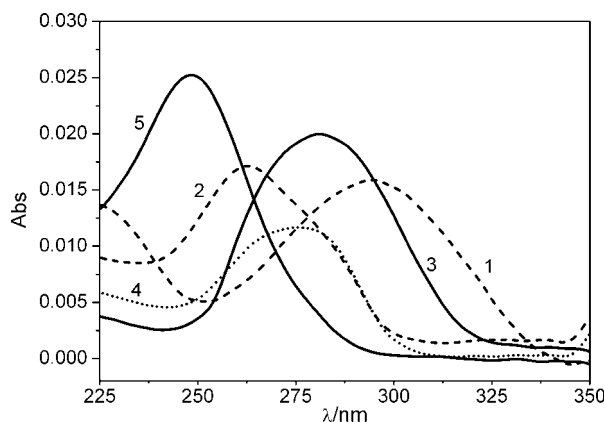


Figure 12. Absorption spectra of the Langmuir films of: 8OCB (1), 8CPB (2), 8CB (3), 8OCFPB (4), and 8OCPFB (5).

Table 4. The position of the absorption maximum, λ_{max} , and the half-bandwidth of the absorption band, δ , for liquid crystals as LB films.

Compound	λ_{max}/nm	$\Delta\lambda_{max} = \pm 1 nm$	δ/cm^{-1}	$\Delta\delta = \pm 50 cm^{-1}$
8CB	281		5700	
5OCB	295		6150	
6OCB	293		6650	
7OCB	293		5750	
8OCB	295		6250	
6CPB	250		6800	
7CPB	249		7050	
8CPB	249		7250	
9CPB	248		7250	
8OCFPB	276		5450	
8OCPFB	264		6600	

Table 5. The position of the absorption maximum, λ_{max} , and the half-bandwidth of the absorption band, δ , and the extinction coefficient, ϵ , for liquid crystals with $n = 8$ dissolved in chloroform at $c = 3.2 \times 10^{-5} mol dm^{-3}$.

Compound	λ_{max}/nm	δ/cm^{-1}	$\epsilon / \frac{dm^3}{mol \cdot cm}$
	$\Delta\lambda_{max} = \pm 1 nm$	$\Delta\delta = \pm 10 cm^{-1}$	$\Delta\epsilon = \pm 100 \frac{dm^3}{mol \cdot cm}$
8CB	283	5180	27,800
8OCB	298	5650	27,200
8CPB	251	5000	31,900
8OCFPB	277	5010	30,700
8OCPFB	263	5900	30,400

absorption transition moments can be considered. This leads to the exciton band splitting given by the formula (34):

$$\Delta E_{NK} = \frac{2|M|^2}{R^3} (1 - 3\cos^2\Theta). \quad (2)$$

M is the electric dipole transition moment of the molecule, R is the centre to centre distance vector between two molecules in dimer, and Θ is the angle between M and R .

When $0^\circ \leq \Theta < 54.7^\circ$, the exciton level is energetically located below the monomer level causing a red shift in the electronic absorption spectrum, and the created aggregates are of the J-type (35). For $54.7^\circ < \Theta \leq 90^\circ$, the exciton band is located energetically above the monomer level causing a blue shift and the creation of H-type aggregates (35). Aggregates corresponding to Θ and having values between 54.7° and 60° are referred to as the intermediate or I-type aggregates (36). The distinct broadening of the absorption band of the liquid crystals investigated as LB films (compared to that characteristic of monomers), with no shift of the absorption maximum position, implies that we are dealing predominantly with the creation of I-aggregates.

In order to quantitatively evaluate the orientation of mesogenic molecules in the LB films, polarised absorption spectra were recorded and the linear dichroism (LD) was determined. Following N'soukpoé-Kossi *et al.* (37) we define LD by:

$$LD = \frac{A_P - A_S}{A_P + A_S}, \quad (3)$$

where A_P and A_S are the absorbance values at the band maximum for the light polarised parallel and perpendicularly to the plane of incidence, respectively.

LD can be related to the angle of incidence, α , in the following way (37):

$$LD_\alpha = \frac{2 - \tan^2\beta}{\tan^2\beta \frac{1 + \cos^2\alpha}{\sin^2\alpha} + 2}, \quad (4)$$

where β is the angle between the transition dipole moment vector and the normal to the plane of the LB film.

Equation (4) is applicable only if there is a homogeneous distribution of the molecule transition moments around the surface normal. In this case the LD for $\alpha = 0^\circ$ should be equal to zero.

Figure 13(a) shows the polarised absorption spectra recorded at $\alpha = 0^\circ$ for 7OCB in the LB film, as an example. It can be seen that, for this liquid crystal, the value of the LD for the light incident perpendicularly to the quartz surface, $LD_\alpha = 0$, is zero. This means that the movement of the quartz slide during deposition did not disturb the homogeneity of the molecular alignment. For other compounds investigated we also obtained $LD_\alpha = 0 = 0$. Thus, the angle β could be calculated from Equation (4) on the basis of the spectra measured at the angle $\alpha \neq 0^\circ$. The spectra of the polarised absorption components recorded at $\alpha = 60^\circ$ for 7OCB are presented in Figure 13(b), and in Table 6 the calculated β angles for the mesogens with $n = 8$ are listed.

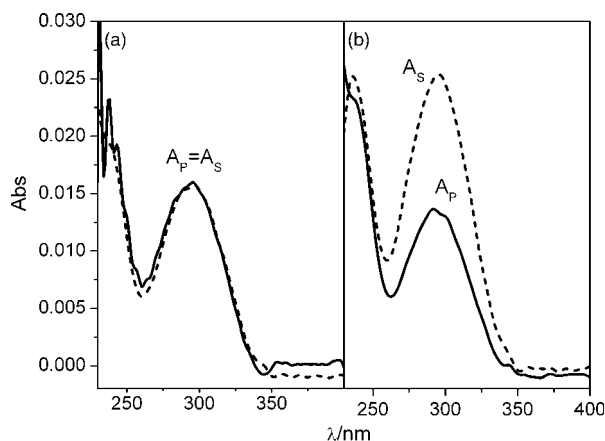


Figure 13. Absorption spectra of the light polarised parallel (A_p) and perpendicularly (A_s) to the incidence plane for 7OCB as LB film. The incidence angle was 0° (a) and 60° (b).

Table 6. Average angles between the rigid molecular cores and the normal to the quartz surface, β for liquid crystals with $n = 8$.

Compound	$\beta/^\circ$
8CB	65
8OCB	60
8CPB	59
8OCFPB	62
8OCFPB	60

On the basis of the β angle we can obtain information about the orientation of the liquid crystal molecules with respect to the normal to slide surface. Knowledge of the angle between the absorption oscillator and the long molecular axis of the liquid crystal is, however, necessary. According to the observed and calculated polarised absorption spectra of such types of mesogens as those from the n CB and n OCB series (38, 39), the electronic transition moment of the main absorption band, occurring in the spectral region used in our experiment and resulting from the $\pi \rightarrow \pi^*$ transition, is assigned to be polarised almost parallel to the long molecular axis (38). For the liquid crystal molecules with the fluorine atom in the lateral position and/or the ester group, this angle can be somewhat larger. However, for the necessity of our considerations, we can assume to a first approximation that the angle between the transition moment direction and the long molecular axis of the mesogens studied here is equal to zero. Thus, the angles β directly reflect the arrangement of the mesogenic molecules in the LB films and for the liquid crystals with $n = 8$ they are collected in Table 6. It is seen that for all the liquid crystals the angle β has a similar value, equal to about 60° . This means that the liquid crystal

molecules are significantly tilted towards the quartz slide surface, in the same way as they are tilted towards the water surface in the Langmuir films. Comparing the values of β (Table 6) and φ (Tables 1–3) it is seen that the rigid cores of the calamitic liquid crystal molecules are significantly more tilted towards the solid surface in the LB films than towards the water in the Langmuir films. This indicates that during the transfer of the monolayer from the air–water interface onto the quartz slide a molecular rearrangement can take place. A similar effect was also observed for other compounds (40–42).

4. Conclusions

The mesogens of several series of thermotropic calamitic liquid crystals have been studied as Langmuir and LB films. The measurements of the surface pressure during the compression process of the Langmuir film have confirmed our previous supposition (13, 42) that liquid crystals with a terminal $-NCS$ group are not able to form a compressible monolayer on the water surface. The mesogenic molecules with very short or very long alkyl or alkoxy chains also do not create Langmuir films, similarly as found previously for liquid crystals from the n CB and n PCH series (14) and for the fatty acid series (3, 4) with varying alkyl chain length.

The surface pressure–area isotherm shape for the Langmuir films of the liquid crystals that make the compressible monolayer at the air–water interface is dependent on the molecular structure of the mesogen rigid core and, to some extent, the chain length. The rigidity of the film shows the tendency to increase with rising chain length, whereas the value of the surface pressure at the collapse point, π_C , remains almost constant. Beyond the collapse point, both π – A and ΔV – A isotherms show a plateau region. The constant value of ΔV in this region suggests that, during the compression, the molecules do not assume more and more vertical alignment, but are ‘pushed out’ above the first monolayer being in contact with the water. Therefore, the effective dipole moment has a physical meaning only up to the collapse point. The value of μ_\perp depends strongly on the liquid crystal molecular structure, indicating that not only the terminal polar group, directly interacting with the water, contributes to it. Other parts of the molecules also have some influence on the resultant value of μ_\perp .

The texture of the Langmuir films has been monitored by BAM. BAM images have revealed that, in the case of nematogens giving stable monolayers, three-dimensional droplet-like domains are formed behind the collapse point. Some indication was also obtained that, in the case of smectogens or their

precursors (e.g. 7OCB), an interdigitated bilayer on the top of the monolayer is formed, similar to that observed by many workers for 8CB (9–12, 14).

The electronic absorption spectra recorded for the liquid crystals as the LB films have revealed that the mesogenic molecules have a tendency to form self-aggregates. The lack of the maximum shift with simultaneous significant broadening of the absorption band of mesogens in the LB films, as compared to the appropriate band in diluted solution, suggests the formation of some fraction of I-type aggregates. The polarised absorption spectra of the LB films have enabled one to calculate the angle between the long molecular axis and the normal to the quartz surface. The value of this angle is rather high, indicating that the mesogenic molecules are significantly tilted with respect to the quartz surface, similarly as to the water in the Langmuir films. The difference between the molecules' tilt angles in both kinds of films indicates that, by the transfer of the floating monolayer on the quartz surface, the rearrangement of molecules occurs. The different tilt of molecules can be, at least partially, due to the surface interactions of the liquid crystal molecules with the solid substrate, which are different than with the water.

Acknowledgements

This work was supported by Poznań University of Technology Research Project No. 64-001/2008 and by MNiSW within the network 'The physical properties of new liquid crystalline materials'.

References

- (1) Bahadur, B., Ed. *Liquid Crystals. Applications and Uses*; World Scientific, Singapore, 1990.
- (2) Jerome, B. *Rep. Prog. Phys.* **1991**, *54*, 391.
- (3) Gaines, G.L. *Insoluble Monolayers at Liquid-Gas Interface*; Interscience: New York, 1996.
- (4) Roberts, G. *Langmuir-Blodgett Films*; Plenum Press: New York, 1990.
- (5) Ulman, A. *An Introduction to Ultrathin Organic Films-from Langmuir-Blodgett to Self-Assembly*; Academic Press: New York, 1991.
- (6) Petty, M.C. *Langmuir-Blodgett Films-An Introduction*; Cambridge University Press: Cambridge, 1996.
- (7) Daniel, M.F.; Lettington, O.C.; Small, S.M. *Thin Solid Films* **1983**, *99*, 61.
- (8) Sakuhara, T.; Nakahara, H.; Fukuda, K. *Thin Solid Films* **1988**, *159*, 345.
- (9) Xue, J.; Jung, C.S.; Kim, M.W. *Phys. Rev. Lett.* **1992**, *69*, 474.
- (10) Friedenber, M.C.; Fuller, G.G.; Frank, C.; Robertson, C.R. *Langmuir*, **1994**, *10*, 1251.
- (11) Janietz, D. *Handbook of Surfaces and Interfaces of Materials*, Nalwa, H.S., Ed.; Academic Press, 2001; pp 423–446; Vol. 1.
- (12) Martyński, T.; Hertmanowski, R.; Bauman, D. *Liq. Cryst.* **2001**, *28*, 437.
- (13) Martyński, T.; Hertmanowski, R.; Bauman, D. *Liq. Cryst.* **2002**, *29*, 99.
- (14) Ingot, K.; Martyński, T.; Bauman, D. *Liq. Cryst.* **2006**, *33*, 855.
- (15) Hoenig, D.; Moebius, D. *J. Phys. Chem.* **1991**, *95*, 4590.
- (16) Hénon, S.; Meunier, J. *Rev. Sci. Instrum.* **1991**, *62*, 936.
- (17) Czupryński, K. *Destabilization of Orthogonal Smectic Phases. Habilitation Dissertation (in Polish)*, Warsaw, 1995.
- (18) Bielejewska, N.; Chrzumnicka, E.; Mykowska, E.; Przybylski, R.; Szybowicz, M.; Władysław, K.; Bauman, D. *Acta Phys. Polon. A* **2006**, *110*, 777.
- (19) Bauman, D.; Wąsik, A.; Jadżyn, J. *Liq. Cryst.* **1996**, *20*, 195.
- (20) Jadżyn, J.; Sokołowska, U.; Déjardin, J.-L. *J. Phys. Chem.* **2008**, *112*, 9050.
- (21) Martyński, T.; Hertmanowski, R.; Dąbrowski, R.; Czupryński, K.; Bauman, D. *Mat. Sci. Engng. C* **2002**, *22*, 105.
- (22) Davies, J.T.; Rideal, E.K. *Interfacial Phenomena*; Academic Press: New York, 1963.
- (23) Myers, D. *Surfaces, Interfaces and Colloids*; Wiley-VCH: New York, 1999.
- (24) Ingot, K.; Martyński, T.; Bauman, D. *Dyes and Pigments* **2009**, *80*, 106.
- (25) Demchak, R.J.; Fort, Jr., T.J. *J. Colloid Interface Sci.* **1974**, *46*, 191.
- (26) Dynarowicz-Łątka, P. *Adv. Colloid Interface Sci.* **1993**, *45*, 215.
- (27) Schmitz, P.; Gruler, H. *Europhys. Lett.* **1995**, *29*, 451.
- (28) Oliveira, Jr., O.N.; Taylor, D.M.; Lewis, T.J.; Salvagno, S.; Stirling, C.J.M. *J. Chem. Soc. Faraday Trans.* **1989**, *85*, 85.
- (29) Taylor, D.M.; Baynes, G.F. *Mat. Sci. Engng. C* **1999**, *8–9*, 65.
- (30) Minkin, V.I.; Osipov, O.A.; Ždanov, Ju.F. *Dipolnye momenty v organiĉeskoj chimiji*; Izdatelstvo Chimija, Moskva, 1968.
- (31) Tamai, N.; Yamazaki, I.; Masuhara, H.; Mataga, N. *Chem. Phys. Lett.* **1984**, *104*, 485.
- (32) David, C.; Bayens-Violant, D. *Mol. Cryst. Liq. Cryst.* **1980**, *59*, 181.
- (33) Itaya, A.; Imamura, T.; Hamaguchi, M.; Miyasaka, H. *Thin Solid Films* **1997**, *292*, 204.
- (34) Kasha, M.; Rawls, H.R.; Ashraf El-Bayoumi, M. *Pure Appl. Chem.* **1965**, *11*, 371.
- (35) Moebius, D. *Adv. Mat.* **1995**, *7*, 437.
- (36) Miyata, A.; Heard, D.; Unuma, Y.; Higashigaki, Y. *Thin Solid Films* **1992**, *210/211*, 175.
- (37) N'Soukpoé-Kossi, Ch.N.; Siewiesiuk, J.; Leblanc, R.M.; Bone, R.A.; Landrum, J.T. *Biochim. Biophys.* **1988**, *940*, 255.
- (38) Wu, S.T.; Ramos, E.; Finkenzer, U. *J. Appl. Phys.* **1990**, *68*, 78.
- (39) Hanemann, T.; Bohn, M.C.; Haase, W.; Wu, S.T. *Liq. Cryst.* **1992**, *11*, 917.
- (40) Hertmanowski, R.; Biadasz, A.; Martyński, T.; Bauman, D. *J. Mol. Structure* **2003**, *646*, 25.
- (41) Biadasz, A.; Martyński, T.; Stolarski, R.; Bauman, D. *Liq. Cryst.* **2006**, *33*, 307.
- (42) Ingot, K.; Kaleta, A.; Martyński, T.; Bauman, D. *Dyes and Pigments* **2008**, *77*, 303.